JOURNAL OF Applied Polymer SCIENCE

Special Issue: Sustainable Polymers and Polymer Science Dedicated to the Life and Work of Richard P. Wool

Guest Editors: Dr Joseph F. Stanzione III (Rowan University, U.S.A.)
and Dr John J. La Scala (U.S. Army Research Laboratory, U.S.A.)

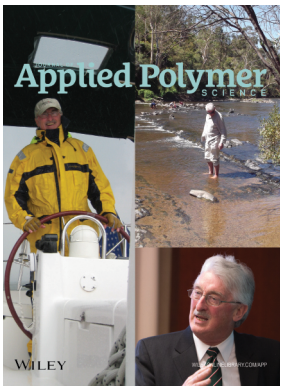

EDITORIAL

REVIEWS

RESEARCH ARTICLES

JOURNAL OF Applied Polymer SCIENCE

Special Issue: Sustainable Polymers and Polymer Science Dedicated to the Life and Work of Richard P. Wool

Guest Editors: Dr Joseph F. Stanzione III (Rowan University, U.S.A.)
and Dr John J. La Scala (U.S. Army Research Laboratory, U.S.A.)

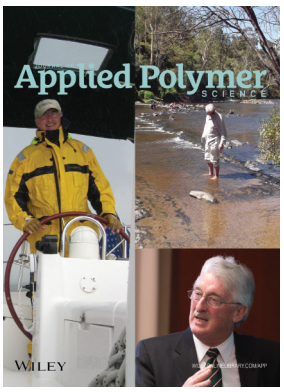

Journal of Applied Polymer Science

Effect of ultrafine talc on crystallization and end-use properties of poly(3-hydroxybutyrate-*co*-3-hydroxyhexanoate)

Jens Vandewijngaarden,[1,2] Marius Murariu,[3] Philippe Dubois,[3] Robert Carleer,[1] Jan Yperman,[1] Jan D'Haen,[4,5] Roos Peeters,[2] Mieke Buntinx[2]

[1]Research Group of Applied and Analytical Chemistry, Hasselt University, Diepenbeek 3590, Belgium
[2]Research Group Packaging Technology Center, IMO-IMOMEC, Hasselt University, Diepenbeek 3590, Belgium
[3]Laboratory of Polymeric and Composite Materials, Center of Innovation and Research in Materials and Polymers (CIRMAP), University of Mons & Materia Nova Research Centre, Mons 7000, Belgium
[4]Institute for Materials Research (IMO), Hasselt University, Diepenbeek 3590, Belgium
[5]IMOMEC, IMEC Vzw, Diepenbeek 3590, Belgium
Correspondence to: M. Buntinx (E-mail: mieke.buntinx@uhasselt.be)

ABSTRACT: Poly(3-hydroxybutyrate-*co*-3-hydroxyhexanoate) (PHBHHx) is a highly versatile polyhydroxyalkanoate. To enhance its slow crystallization, the performance of ultra-fine talc (median diameter of 1 μm) as a nucleating agent is studied. This study focuses on crystallization, but also on the effect on fundamental properties (i.e., thermal stability) and selected end-use properties (i.e., color, opacity, tensile properties, and gas permeability), to assess its applicability for food packaging purposes. Samples containing 0.5, 1, and 2 wt % were prepared through melt blending and compression molding. First, it was proven that ultra-fine talc is a highly performant nucleating agent for PHBHHx. The isothermal crystallization half time at 70 °C was reduced to 97% by adding 2 wt % of talc, which could greatly improve the processability of PHBHHx. Thermal stability increased with 3–4 °C, due to increased barrier effect. Permeability for O_2, CO_2, and water vapor increased slightly upon addition of 0.5 wt % and 1 wt % talc, but decreased at 2 wt % talc. Nevertheless, the results remained within the same applicability range. An acceptable total color change of 0.9 was observed. Furthermore, the PHBHHx matrix was rendered stiffer (Young's modulus increased with 100 MPa), while showing hardly any change in elongation at break or tensile strength. Overall, it can be concluded that ultrafine talc is a very efficient nucleating agent for PHBHHx. Besides the beneficial effect on crystallization, the ultrafine talc hardly influenced any other property, which could prove to be of high added value for the application of these composites as food packaging material. © 2016 Wiley Periodicals, Inc. J. Appl. Polym. Sci. **2016**, *133*, 43808.

KEYWORDS: biopolymers & renewable polymers; composites; crystallization; packaging

Received 16 December 2015; accepted 12 April 2016
DOI: 10.1002/app.43808

INTRODUCTION

Polyhydroxyalkanoates (PHAs) are a family of biobased polymers that have received a great deal of attention the last few decades for certain applications, such as packaging, medical devices, and controlled drug-delivery systems.[1,2] PHAs are polyesters, that can be produced by a variety of bacteria from a wide range of renewable organic substrates.[3] These polyesters are biodegradable as well as biocompatible.[4]

Poly(3-hydroxybutyrate-*co*-3-hydroxyhexanoate) (PHBHHx) can be considered as a candidate for replacement of specific fossil-based polymers, due to its ductile nature and wider processing window, compared to poly(3-hydroxybutyrate) (PHB) and poly(3-hydroxybutyrate-*co*-3-hydroxyvalerate) (PHBV), which are the two most investigated PHAs.[5–7] The mechanical properties of PHBHHx have been compared to low-density polyethylene,[8,9] with a possible application for packaging.[8,10]

Unfortunately, the crystallization rate of PHBHHx is very slow, even at low 3-hydroxyhexanoate content. Therefore, many efforts are actually devoted to solve this problem (e.g., by addition of a nucleating agent or selected microfillers or nanofillers).[11,12] Talc is a layered silicate, which has excellent nucleating properties for conventional polymers, such as polypropylene[13,14] and poly(ethylene terephthalate),[15] by providing a foreign surface for nuclei to grow on. Talc is a phyllosilicate with ideal

chemical formula $Mg_3Si_4O_{10}(OH)_2$.[16,17] It is a crystalline layered silicate without charge and thus without interlayer cations. Talc possesses a trioctaedric structure, comprised of three hydrated layers. The elemental layer is an octahedral plane, composed of linked $[MgO_4(OH)_2]^{8-}$ octahedrons. This layer is confined between two tetrahedral sheets of linked $(SiO_4)^{4-}$ tetrahedrons.[17] Talc is made up of stacks of the triple-sheet crystalline units, which are held together by Van der Waals forces between surface oxygen atoms.[18]

It has been shown that talc enhances crystallization of PHB, PHBV,[19,20] and poly(3-hydroxybutyrate-*co*−4-hydroxybutyrate)[21] at concentrations lower than 5 wt % as well. In these studies, only the crystallization properties were characterized in-depth, whereas end-use properties were left untouched. Moreover, it has been shown that better properties can be obtained with lower concentrations of ultra-fine talc in comparison to larger particle size talc. This has been observed for several polymeric systems, such as polypropylene,[22] poly(lactic acid),[23,24] and polycarbonate/poly(butylene terephthalate) blends.[25] Petchwattana *et al.* (2014) have studied the effects of up to 10 wt % talc in promoting the crystallization of poly(lactic acid) (PLA). Three different talc particle sizes, namely 1, 5, and 30 μm, were used as nucleating agent. Talc was found to be an effective nucleating agent for accelerating the crystallization rate in PLA, whereas the finer talc particles were found to lead slightly to higher degrees of crystallinity.[23]

A few studies have been done regarding the addition of submicron- or nanosized inorganic particles to a PHBHHx matrix,[11,26–29] however a significant improvement in crystallization properties has not yet been reported. Xie *et al.* (2009) observed slight increases (at concentrations ≤ 3 wt %) and decreases (at concentrations ≥ 3 wt %), of the order of 5 °C–10 °C, in crystallization peak temperature upon addition of silica nanospheres and -fibers.[29] A recent study by the authors regarding PHBHHx/organomodified montmorillonite nanocomposites revealed a negative influence on the crystallization properties.[26]

In this study, a novel grade of ultra-fine talc (median diameter of 1 μm) was selected and combined with a PHBHHx matrix through melt blending and compression molding. Besides, the effect of the addition of ultra-fine talc on fundamental properties (i.e., thermal stability and crystallization) of PHBHHx, packaging properties such as gas permeability, tensile properties, color, and opacity are investigated as well, which is often not included in other studies.

EXPERIMENTAL

Materials and Sample Preparation

Pure PHBHHx powder, with a 3-hydroxyhexanoate content of 10.5 mol %, was provided by Kaneka Corporation (Westerlo-Oevel, Belgium) and dried at 70 °C *in vacuo* for 3 days.

Ultra-fine talc powder, tradename Jetfine® 3CA, was kindly provided by Imerys Talc (Gent, Belgium). According to the technical sheet, the median diameter d_{50} of the talc particles was 1 μm, as measured by sedimental analysis. The powder was dried at 120 °C for 1 day prior to use. Samples containing 0.5, 1, and 2 wt % were prepared, along with a reference sample containing no talc.

First, samples with a total weight of 55 g were dry-mixed in a Rondol mini-mix high speed mixer, before being processed in a Brabender counter-rotating internal mixer equipped with roller blades at a temperature of 140 °C. During feeding of the mixer, a rotation speed of 30 rpm was used for 3 min to avoid the excessive increase of the torque during polymer melting. Then the rotation speed was increased to 70 rpm for 8 min.

Subsequently, samples of about 1.8 g were compressed and molded at 140 °C to prepare films in a polyimide mold (100 mm × 100 mm × 0.150 mm) using an Agila PE20 hydraulic press. The polymer was preheated for 90 s without pressure, after which it was pressed at 30 bar for 150 s, followed by three degassing cycles. Finally, the films were pressed at high pressure of 150 bar for 120 s, followed by a slow cooling at 50 bar for 20 min at 60 °C to allow film crystallization and easy demolding.[30]

Thicker samples for tensile testing were produced in a stainless steel mold (100 mm × 100 mm × 0.5 mm) at 140 °C with a pre-heating time of 3 min before being pressed at 30 bar for 200 s. Subsequently, two 3 s degassing cycles were used before finally molding the sample at 150 bar for 150 s. The samples were slowly cooled at 50 bar for 20 min at 60 °C.

Differential Scanning Calorimetry

Thermal properties of the prepared films were analyzed in sealed aluminum pans under inert atmosphere (50 mL/min nitrogen) using a TA Instruments Q200 differential scanning calorimeter (DSC) and sample weights of about 3.5 mg.

For non-isothermal crystallization experiments, the sample was heated from −30 °C to 170 °C at a heating rate of 10 °C/min. After being kept isothermal for 2 min, the sample was cooled at 10 °C/min to −30 °C and kept constant for 2 min prior to heating to 170 °C at 10 °C/min.

For isothermal crystallization experiments, the sample was heated from −30 °C to 170 °C at a heating rate of 10 °C/min. After an isothermal period of 3 min, the sample was rapidly cooled to 70 °C at 45 °C/min and kept isothermal until crystallization was completed.

For all samples, only the weight fraction of polymer in the composites was considered to allow a more accurate determination of enthalpy values. Measurements were performed at least twice.

Polarized Optical Microscopy

Polarized optical microscopy (POM) experiments were performed using a Nikon Optiphot-Pol polarized optical microscope. Solutions of 5 mg/mL of each sample in chloroform were prepared. A few drops were placed on a microscopy glass and left to dry for 5 min before being placed for 1 day in a vacuum oven at 70 °C. After drying, each sample was isothermally crystallized, using a DSC oven, in the following way: heating to 170 °C at 10 °C/min, isothermal period at 170 °C for 10 min, cooling to 70 °C at 45 °C/min, and finally isothermal crystallization for 40 min at 70 °C.

Transmission Electron Microscopy

The transmission electron microscopy (TEM) study was performed with a FEI Tecnai Spirit using an accelerating voltage of 120 kV. The images are standard BF (bright field) images.

Transparent slices of about 150-nm thick are made with a Leica EM UC6 ultramicrotome.

Gel Permeation Chromatography

The molecular weight distribution of the samples was analyzed using a gel permeation chromatography (GPC) apparatus composed of a SpectroSeries P100 pump, equipped with a Shodex RI71 refractometer detector and two PL-gel 10 µm Mixed-B columns in series, thermostated at 35 °C. The eluent was chloroform (VWR, HPLC grade) at a flow rate of 1.0 mL/min. Samples were dissolved in chloroform at a concentration of 1 g/L and filtered over a 0.45-µm syringe filter. The injection volume was 100 µL. Calibration was performed using polystyrene standards (474–3150 $\times$ 10^3 g/mol) dissolved in chloroform with a concentration of 1 g/L.

Thermogravimetric Analysis

The thermal stability of the samples was analyzed using a TA Instruments Hi-Res TGA 2950 thermogravimetric analyser. Samples of about 10 mg were heated from room temperature to 350 °C at a heating rate of 20 °C/min with a N_2 gas flow of 80 mL/min. Measurements were performed at least in duplicate.

Colorimetric Analysis

Colorimetric analysis was performed using a Datacolor Micro-Flash 200d. Results are presented in CIELAB color coordinates ($L^\star$, $a^\star$, and $b^\star$). The total color change ΔE_{ab} is calculated as:

$$\Delta E_{ab} = \sqrt{\Delta L + \Delta a^2 + \Delta b^2} \quad (1)$$

with ΔL, Δa, and Δb, respectively, the difference in $L^\star$, $a^\star$, and $b^\star$ between the reference (0% talc) and the samples containing talc. $L^\star$, $a^\star$, and $b^\star$ represent degree of lightness, red/green, and blue/yellow, respectively. Measurements were performed in duplicate.

Opacity

The opacity of the prepared films was determined according to the Hunter Lab method in the reflectance mode, using a Datacolor Microflash 100D. The opacity Y (in %) can be calculated as the relationship between the opacity of a sample on a black standard Y_b and the opacity on a white standard Y_w:

$$Y = Y_b / Y_w \times 100 \quad (2)$$

Each sample was measured four times (twice on each side).

Gas Permeability

The oxygen transmission rate (OTR), at 23 °C and 0% relative humidity (RH), of the produced samples was measured using a Mocon Ox-Tran 702 (ASTM D3985). Carbon dioxide transmission rate (CO_2TR) at 23 °C and 0% RH was measured using a Mocon Permatran-C 4/41 (ASTM F2476). Water vapor transmission rate (WVTR) was measured using a Mocon Permatran-W 700 (ASTM F1249). Test gases (O_2 and CO_2) and carrier gas (N_2 or N_2/H_2) with a purity of 99.999% were purchased from Westfalen (Germany). Samples were placed between 2 aluminum masks with an effective testing area of 5 cm^2. The sample was exposed to the test gas on one side and to a continuously flushing carrier gas on the other side, both at a total pressure of 1 atm. The test gas diffuses through the sample and is guided by the carrier gas toward the detector. The gas transmission rate or gas flux J, in cm^3/m^2 day atm (for OTR and CO_2TR) or g/m^2 day (for WVTR) of the specific test gas, is reported when equilibrium is reached (i.e., the concentration of test gas in the carrier gas changes less than 1% during a test cycle of 30 min). The gas flux J can be defined as the quantity of test gas or permeant Q, which passes through the polymeric film per unit area A during one unit of time t at equilibrium[31–33]:

$$J = Q/(A.t) \quad (3)$$

In order to obtain a thickness-independent criterion for comparison, the gas flux J can be normalized for sample thickness d and permeant pressure p to obtain the permeability coefficient P[31–33]:

$$P = J.d/p \quad (4)$$

Sample thickness was measured prior to permeability testing using a MTS MI20 thickness gauge. The thickness was taken as the average of five measurements at different locations of each sample.

For each sample, the gas permeability of two specimens was measured in duplicate.

Tensile Testing

The tensile test was performed according to ASTM D638-02 using a MTS/10 tensile tester at a crosshead speed of 1 mm/min and a distance of 25.4 mm between the grips. Samples were cut into dumbbell shapes (ASTM D638-02 type V) and were conditioned at 23 °C and 50% relative humidity for 48 h before testing. At least 10 specimens were tested for each sample.

RESULTS AND DISCUSSION

Crystallization Properties

For the non-isothermal crystallization experiments, the most important parameters related to crystallization, that can be derived, are the onset temperature of crystallization ($T_{c,o}$), crystallization peak temperature ($T_{c,p}$), and the crystallization enthalpy (ΔH_c). The difference between $T_{c,o}$ and $T_{c,p}$ is calculated as well for each sample in order to observe any changes in crystallization peak width. These results are presented in Table I. The non-isothermal crystallization curves are given in Figure 1(A). Upon cooling from the molten state at 170 °C, pure PHBHHx does not display any significant crystallization behavior. However, upon addition of ultra-fine talc, an outspoken crystallization peak can be observed. It is also clear that $T_{c,o}$ and $T_{c,p}$ are raised to higher temperatures with increasing amounts of talc. Adding 0.5 wt % talc results in a $T_{c,p}$ of 65.9 °C, whereas $T_{c,p}$ is 70.3 °C for 2 wt % talc. Pure PHBHHx also presents cold crystallization during subsequent heating (onset temperature and enthalpy of 54.1 °C and 6.3 J/g, respectively), whereas the samples containing talc do not present any kind of cold crystallization behavior under these testing conditions. This is also a clear indication of the higher crystallinity achieved during cooling from the melt, with ΔH_c being about 33 J/g for the samples containing talc. From these non-isothermal DSC experiments, it is very clear that talc acts as a nucleating agent[19] and thus promotes crystallization of PHBHHx. The crystallization enthalpy ΔH_c is constant for all samples containing talc. Important to note is that the width of the crystallization peak ($T_{c,o} - T_{c,p}$) decreases slightly from 7.7 to 7.1 °C, for

Table I. Non-Isothermal and Isothermal Crystallization Properties of PHBHHx/talc Composites (n.d. = not detected)

Talc content	$T_{c,o}$ (± 0.1 °C)	$T_{c,p}$ (± 0.1 °C)	ΔH_c (± 0.5 J/g)	$T_{c,o} - T_{c,p}$ (°C)	$t_{1/2}$ (± 0.04 min)
0 wt %	n.d.	n.d.	n.d.	n.d.	15.28
0.5 wt %	73.5	65.9	33.6	7.6	1.54
1 wt %	75.4	68.1	33.8	7.3	0.52
2 wt %	77.4	70.3	32.9	7.1	0.44

respectively 0.5 and 2 wt %, which is indicative of faster crystallization.

In order to gain more insights into the effect of talc on the crystallization properties of PHBHHx, isothermal crystallization experiments were performed as well. From isothermal crystallization at 70 °C, the crystallization half-time $t_{1/2}$ (time needed to reach 50% relative crystallinity) is calculated. The crystallization half-time $t_{1/2}$ is presented in the right-hand side of Table I. The DSC curves are presented in Figure 1(B).

Pure PHBHHx (top curve) displays a very broad and weak crystallization peak, corresponding to a high $t_{1/2}$ of 15.28 min. The addition of ultra-fine talc dramatically reduces $t_{1/2}$ to only a fraction of neat PHBHHx. A talc content of 0.5, 1, and 2 wt % leads to a $t_{1/2}$ of 1.54, 0.52, and 0.44 min, respectively, which corresponds to reduction of up to 97% and an increasingly narrow crystallization peak. The isothermal experiments clearly display that the addition of talc to PHBHHx, even in low concentrations (0.5 wt %) is highly beneficial for the crystallization properties. These experiments also further clarify the importance of talc concentrations. By adding 1 wt % talc, the value of $t_{1/2}$ is only one-third of $t_{1/2}$ at a concentration of 0.5 wt %. Increasing the talc content to 2 wt % has a slightly lower $t_{1/2}$, but the effect is not as outspoken. Ultra-fine talc particles show a similar efficiency as cyanuric acid[34] and uracil,[35] which were proven to be highly efficient by reducing $t_{1/2}$ with about 95% at a concentration of 1 wt %.

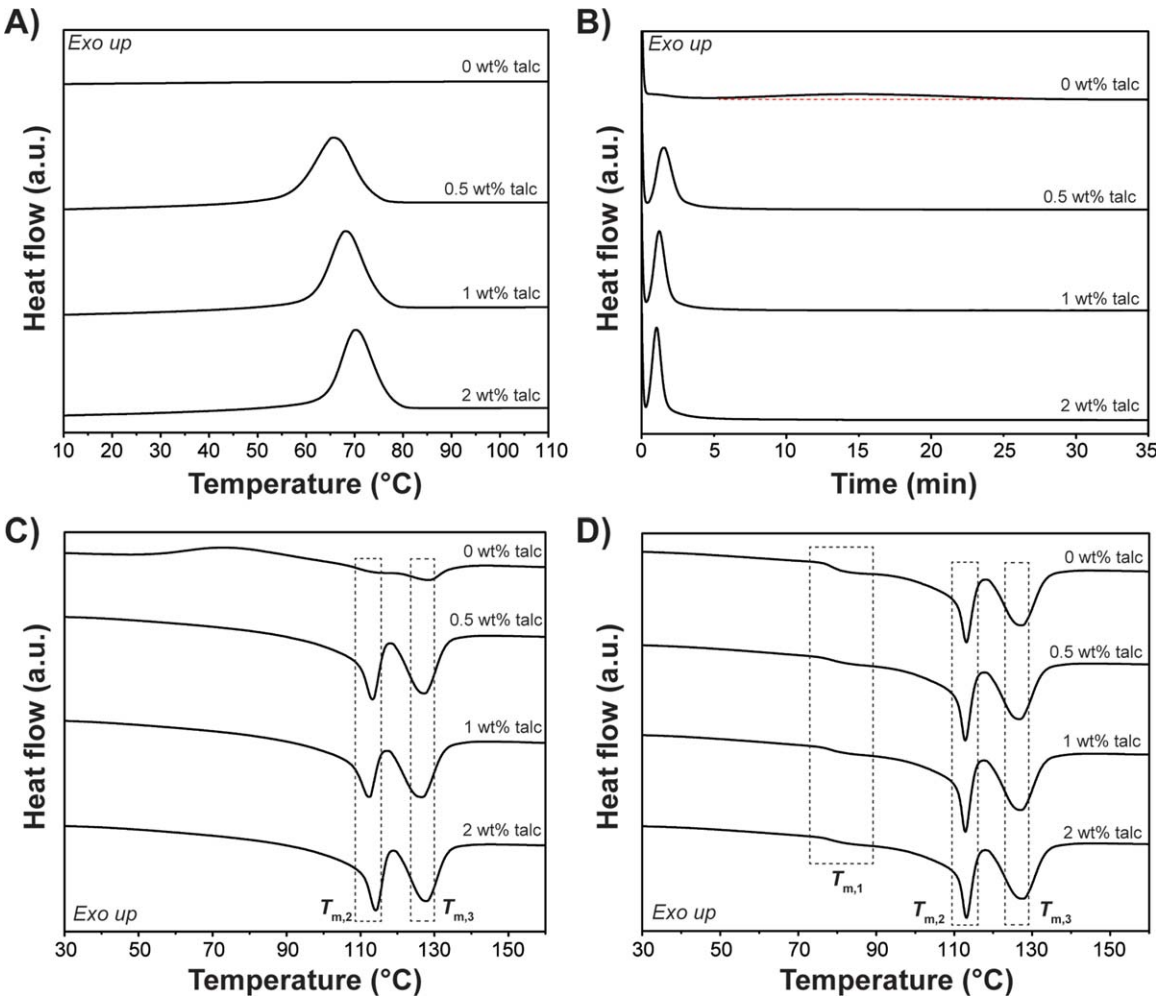

Figure 1. DSC curves of (A) non-isothermal crystallization, (B) isothermal crystallization, (C) melting after non-isothermal crystallization, and (D) melting after isothermal crystallization of PHBHHx/talc composites. [Color figure can be viewed in the online issue, which is available at wileyonlinelibrary.com.]

Table II. Melting Behavior after Non-Isothermal and Isothermal Crystallization from the Molten State (n.d. = not detected)

Talc content	$T_{m,1}$ (± 0.3°C)	$T_{m,2}$ (± 0.4°C)	$T_{m,3}$ (± 0.3°C)
After non-isothermal crystallization:			
0 wt %	n.d.	114.6	128.2
0.5 wt %	n.d.	112.3	126.9
1 wt %	n.d.	113.3	127.2
2 wt %	n.d.	114.1	127.7
After isothermal crystallization:			
0 wt %	81.8	113.1	127.1
0.5 wt %	82.6	112.8	127.6
1 wt %	81.8	112.8	127.0
2 wt %	82.0	113.1	127.3

The melting behavior subsequent to non-isothermal and isothermal crystallization was investigated as well. The DSC curves are given in Figure 1(C,D) and the corresponding peak temperatures are given in Table II. All samples show two endothermal peaks related to melting, designated as $T_{m,2}$ and $T_{m,3}$ during melting after non-isothermal crystallization. The peak at lower temperature is related to the melting of primary lamellae, whereas the peak at higher temperature is due to melting of lamellae, which have been formed through reorganization or thickening during DSC heating.[36] For the pure PHBHHx sample an exothermal peak at 73.3 °C is observed and can be attributed to cold crystallization (crystallization enthalpy of 5.1 J/g), due to incomplete crystallization in the previous cooling step. It is clear that the presence of ultra-fine talc has an outspoken influence on the melting behavior after non-isothermal crystallization. Even though the melting peak temperatures are not significantly altered, the melting peaks are much sharper and more outspoken for the samples containing talc, indicative of more stable and uniform crystallites. Cold crystallization is also completely eliminated in the presence of ultra-fine talc. During melting after isothermal crystallization a new peak at ~82 °C is observed, which is due to melting of secondary crystallites formed during isothermal crystallization.[36] In general, the melting behavior after isothermal crystallization is not significantly influenced by the presence of ultra-fine talc particles.

In order to assess the effect of ultra-fine talc on spherulite size of PHBHHx, some polarized optical microscopy experiments were performed. These images are presented in Figure 2 at a 20× magnification. The differences in spherulite size can be discerned immediately. Pure PHBHHx presents very large spherulites, with diameters ranging between ~100 and 150 μm. The addition of talc in all tested concentrations, results in a much larger number of smaller spherulites, with a diameter of ~20 μm.

By combining DSC experiments with POM, it can be concluded that ultra-fine talc is a highly performant nucleating agent for PHBHHx containing 10.5 mol % 3-hydroxyhexanoate units. This is in contradiction with the study performed by Jacquel *et al.* (2010), in which talc appeared to have no significant effect on the crystallization of a similar type of PHBHHx. Unfortunately, the particle size of the talc was not disclosed, so it is not possible to make a direct comparison. One must also consider that the studied composites were prepared by solvent casting.[37] In this study however, the samples were prepared by dry-mixing followed by melt compounding, which could play a key role in determining the final properties. The above results, however, clearly show the enhanced crystallization properties of the samples at hand. An important parameter to keep in mind is the effect of particle size. In this study, only one size of ultra-fine talc was employed. However, it is plausible that further reduction of particle size could lead to even better crystallization properties, or similar crystallization properties but at lower filler concentrations. This has also been proven to be the case of PLA nucleated with ultra-fine talc with different particle sizes.[23]

Dispersion Study

A dispersion study of ultra-fine talc particles in the PHBHHx matrix was performed using TEM. These images are given in Figure 3. After observation in multiple locations of several microtome cuts, it is clear that for all three samples containing ultra-fine talc, a rather homogeneous dispersion of inorganic particles (dark) was observed. It can also be clearly seen that the particle size distribution of the ultra-fine talc is rather broad, ranging from a few microns to submicron particles.

Thermal Degradation during Processing

Using GPC, the thermo-mechanical degradation occurring during melt blending of the polymer and talc was investigated. The number average molecular weight $\bar{M}_n$, weight average molecular weight $\bar{M}_w$, and dispersity ($Đ_M$), defined as the ratio of $\bar{M}_w$ to $\bar{M}_n$, were determined before (virgin) and after melt processing. These results are presented in Table III. It becomes immediately clear that melt processing induces a significant decrease in molecular weight, due to thermal and shear-induced degradation. Upon comparison of the composites, it is possible to observe some fluctuation in results, however no correlation between the talc content and reduction in molecular weight is found. Thus, it must be concluded that the presence of the ultra-fine talc particles during melt processing will not induce a significant amount of extra polymer degradation. It is also important to note that typically the processing itself does not seem to affect the dispersity severely, despite the significant reduction in $\bar{M}_w$ and $\bar{M}_n$.

Thermal Stability

The thermal stability of the prepared composites was investigated using thermogravimetric analysis (TGA) under pure nitrogen atmosphere from room temperature to 350 °C with a heating rate of 20 °C/min. Useful key parameters determined from TGA results are the onset temperature of degradation T_o, calculated as the intersection of the extrapolated initial base line and the tangent to the inflection point; T_{50} (temperature at 50% weight loss of polymer matrix) and T_{max}, which is the temperature at which the rate of weight loss is the highest.

These results are presented in Table IV. It can be observed that all three indicative parameters increase slightly at higher talc contents, thus implying a higher thermal stability. The addition of 2 wt % talc to PHBHHx leads to the greatest effect, increasing T_o, T_{50}, and T_{max} with 4.0 °C, 3.6 °C, and 2.5 °C, respectively.

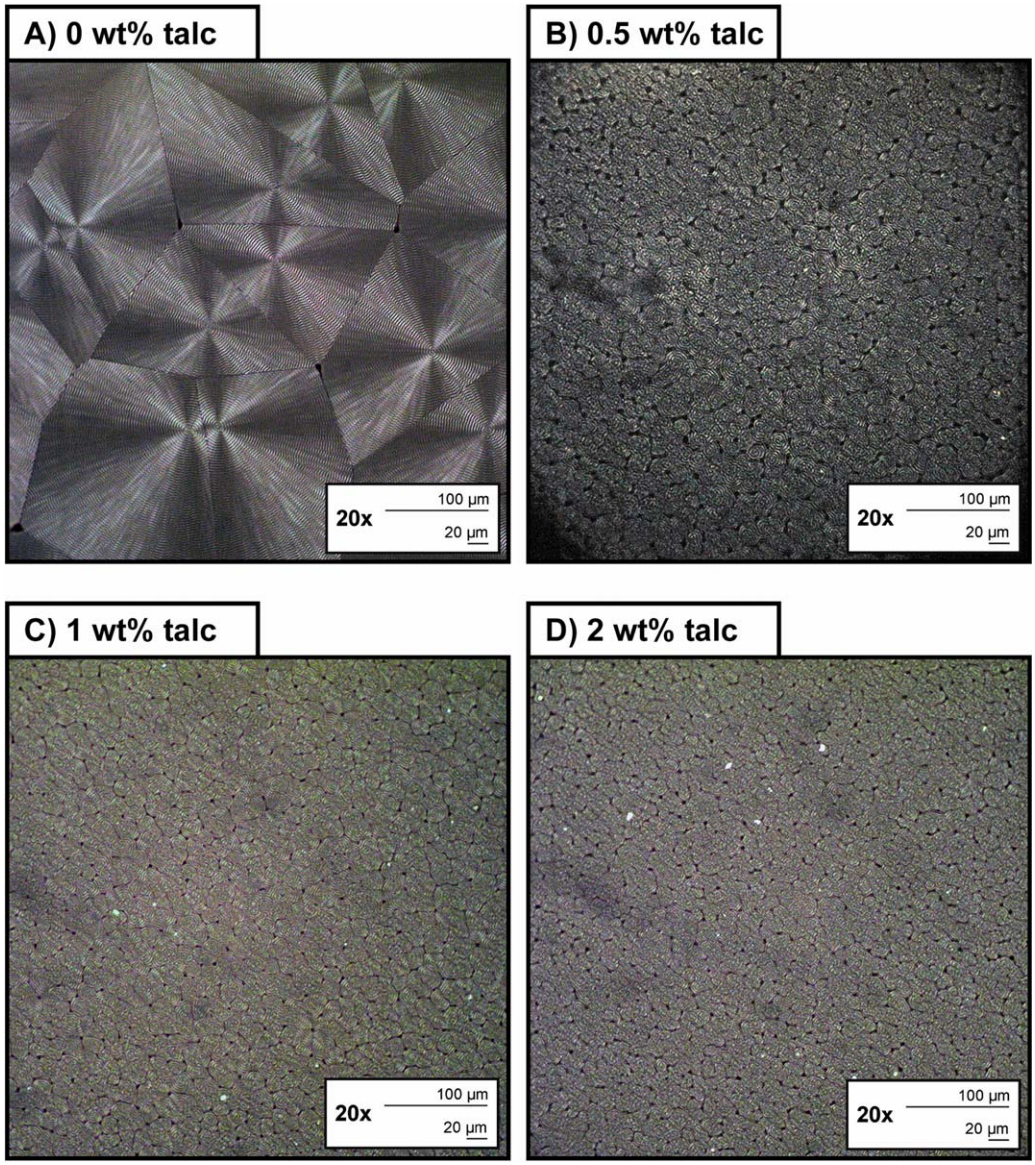

Figure 2. POM images of PHBHHx/talc composites containing (A) 0 wt %, (B) 0.5 wt %, (C) 1 wt %, and (D) 2 wt % of ultra-fine talc. [Color figure can be viewed in the online issue, which is available at wileyonlinelibrary.com.]

Zhang *et al.* (2007) observed a slight increase of 4 °C in T_{max} in solvent cast PHBHHx samples containing 3 wt % talc,[11] similar to the results presented in this study. An increase in thermal stability due to the presence of talc in the polymer matrix has also been observed in other polymeric systems, such as poly(lactid acid)/poly(ε-caprolactone) blends[38] and poly(butylene succinate).[39] In both studies, this increase in stability was attributed to the so-called barrier effect, due to the fact that the presence of an inorganic filler (having a platelet morphology in this study) hinders the release of volatile degradation products by creating a tortuous path.

Colorimetric Analysis and Opacity

The change in color coordinates (ΔL, Δa, and Δb) and the total color change (ΔE_{ab}) of the prepared samples are presented in Table V, with neat PHBHHx used as a reference to calculate color change upon addition of talc. The impact of talc on the colorimetric properties of PHBHHx is rather limited, with ΔL becoming more negative upon increasing the amount of talc, indicative of the samples becoming slightly darker. Δb is positive and increasing with higher talc loading, implying more yellowness. The total color change ΔE_{ab} is only limited, reaching a maximum value of 0.9 for 2 wt % talc. For further clarification of these results, one must comprehend that ΔL, Δa, and Δb must be at least 0.1 to be considered as a color change. Moreover, in quality control circumstances a total color change ΔE_{ab} of 2 is still considered as acceptable, whereas in this study a ΔE_{ab} of only 0.9 is observed.

The results of the opacity measurements are given in the right-hand column of Table V. It can be concluded that the samples are rendered slightly more opaque upon addition of increasing amounts of talc. This can be expected because foreign particles are introduced in increased concentration, which can reflect

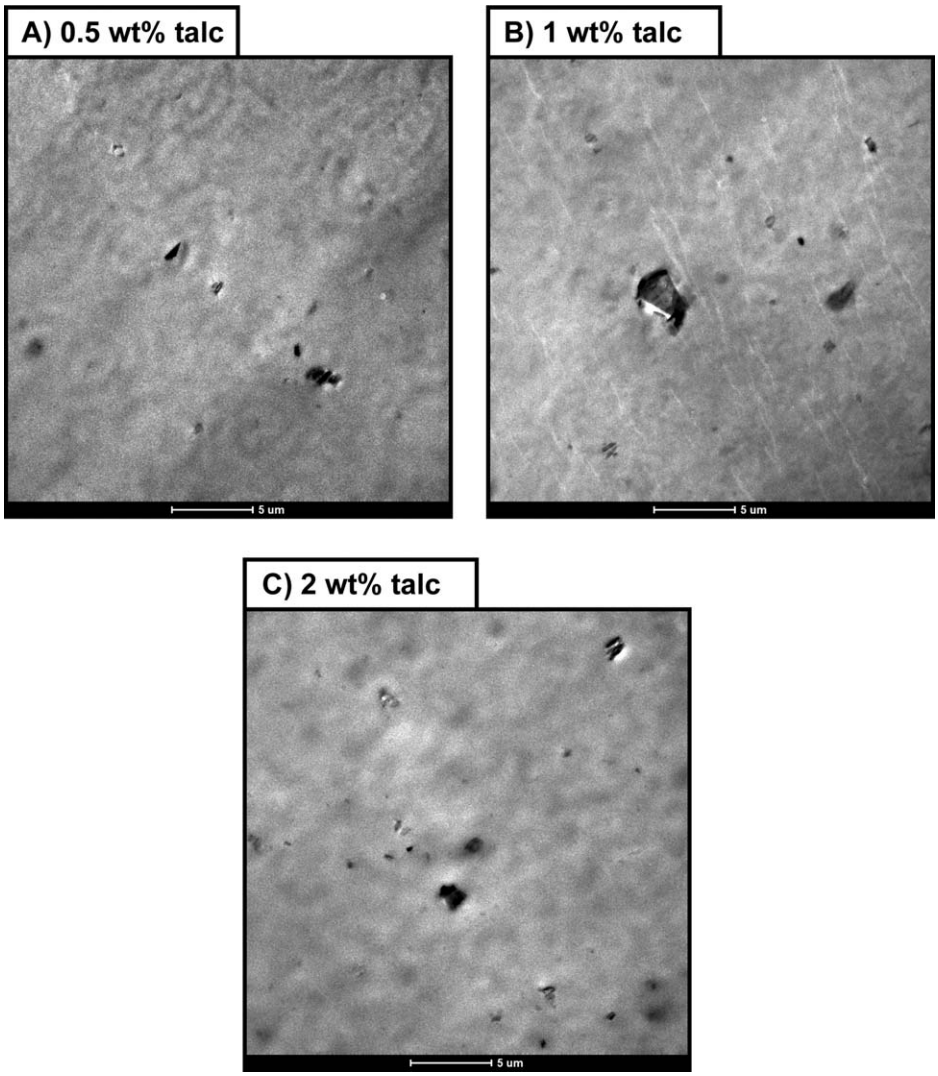

Figure 3. TEM images of PHBHHx samples with ultra-fine talc concentrations of (A) 0.5 wt %, (B) 1 wt %, and (C) 2 wt %.

light and thus induce opacity. However, this effect is not very extensive, as the opacity increases from 10% to only 13.9% at a talc loading of 2 wt %.

Barrier Properties

The barrier properties, with relevance for packaging applications, were investigated through analysis of permeability of the produced samples for oxygen, carbon dioxide, and water vapor (PO_2, PCO_2, and PH_2O). The results are presented in Table VI. The permeability coefficients of the neat PHBHHx film are fairly similar to the ones previously published by the authors, remaining within the same range of applicability.[36] Since the talc particles in the PHBHHx matrix can be considered as physically impermeable to gas or vapor molecules, a reduction in gas permeability due to creation of an enhanced tortuous path was initially expected, with the filler amount being a key parameter that must be taken into account. However, upon addition of 0.5 wt % talc, the values for PO_2, PCO_2, and PH_2O, unexpectedly, were slightly increased. By increasing the talc content further to 1 and 2 wt %, PO_2, PCO_2, and PH_2O start to decrease again, with the 2 wt % sample performing slightly better than the neat PHBHHx. Lastly, it is noteworthy to mention that the

Table III. Molecular Weight Distribution of PHBHHx/Talc Composites

Talc content	$\bar{M}_n$ ($\times 10^3$ g/mol)	$\bar{M}_w$ ($\times 10^3$ g/mol)	$Đ_M$
virgin PHBHHx	272	686	2.5
0 wt %	179	489	2.7
0.5 wt %	176	525	3.0
1 wt %	222	523	2.4
2 wt %	194	488	2.5

Table IV. Thermal Properties of PHBHHx/talc Composites

Talc content	T_o (°C)	T_{50} (°C)	T_{max} (°C)
0 wt %	288.9 (±0.2)	300.7 (±0.2)	307.6 (±0.1)
0.5 wt %	289.9 (±0.3)	301.8 (±0.5)	306.5 (±0.7)
1 wt %	292.9 (±0.8)	304.2 (±0.2)	310.1 (±0.4)
2 wt %	292.9 (±0.1)	304.3 (±0.3)	310.1 (±1.6)

Table V. Colorimetric Properties and Opacity of PHBHHx/talc Composites

Talc content	ΔL	Δa	Δb	ΔE_{ab}	Opacity Y (± 0.2%)
0 wt %	/	/	/	/	10.0
0.5 wt %	−0.2	0	0	0.2	10.3
1 wt %	−0.2	0	0	0.2	11.1
2 wt %	−0.8	0	0.4	0.9	13.9

Table VI. Gas Permeability Properties of PHBHHx/talc Composites

Talc content	PO_2 (cm^3 mm/m^2 day atm)	PCO_2 (cm^3 mm/m^2 day atm^1)	PH_2O (g mm/m^2 day)
0 wt %	7.9 (± 0.2)	37.0 (± 0.7)	1.27 (± 0.01)
0.5 wt %	9.0 (± 0.7)	41.9 (± 0.4)	1.54 (± 0.09)
1 wt %	8.4 (± 0.2)	39.9 (± 0.9)	1.32 (± 0.04)
2 wt %	7.5 (± 0.2)	38.6 (± 0.7)	1.21 (± 0.05)

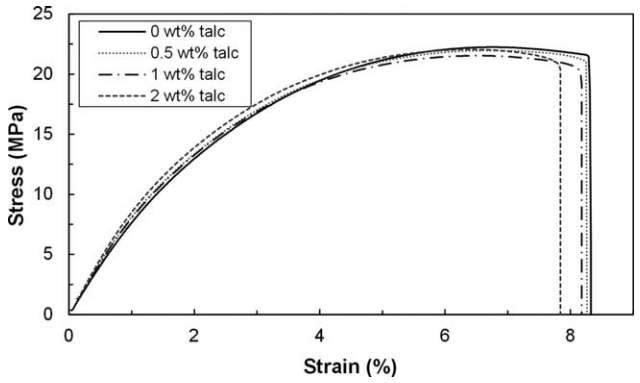

Figure 4. Examples of stress–strain curves of PHBHHx/talc composites with 0–2 wt % talc. [Color figure can be viewed in the online issue, which is available at www.wileyonlinelibrary.com.]

literature information about the effects of talc addition in different polymer systems is somewhat contradictory, but in many cases a significant improvement of gas and water vapor barrier properties is reported (e.g., in PLA-talc based composites[38]). We suspect also that under typical extrusion conditions the improvements in barrier properties of PHBHHx—talc films are to be even more obvious with respect to neat PHBHHx films: (a) owing to the effectiveness of the nucleating agent which leads to uniform microcrystalline structure and higher crystallinity, (b) due to possible orientation of talc platelets following the extrusion and drawing process.

A possible explanation for this trend might be related to the enhanced nucleation, induced by the ultra-fine talc particles in the PHBHHx matrix. It is well known that the addition of a nucleating agent results in the formation of a larger amount of nuclei, which will finally grow into crystallites.[19] However, due to the higher number of crystallites, they will be significantly smaller in size, in comparison to the lower amount of larger crystallites formed in a non-nucleated polymer. This effect was clearly shown in Figure 2. The crystalline fraction of the polymer acts as a barrier to gas permeability, but if the crystallites are smaller, the tortuous path is reduced as well, which is the case for the sample containing 0.5 wt % talc. Upon increasing the talc content, a second phenomenon comes into play. The physical impermeability of the talc platelets will become more important than the reduced crystallite size, which could explain the subsequent reduction in gas permeability at higher talc concentrations.

Tensile Properties

In order to assess the effect of a variable concentration of ultra-fine talc on the tensile properties, stress–strain curves were measured, as shown in Figure 4. From these measurements, it is possible to determine Young's modulus, tensile strength (calculated from the maximum in load), the nominal strain at break, and the nominal strain at the point of maximum load, which are presented in Table VII. From these results, it can be concluded that adding small amounts of ultra-fine talc has only a limited effect on the tensile properties. The maximum tensile strength stays constant, whereas the nominal strain at maximum load and nominal strain at break show a decreasing trend, though very limited. The most outspoken change can be found in the Young's modulus, which increases gradually from 804 MPa to 907 MPa upon addition of 2 wt % talc. Globally, the addition of ultra-fine talc, with a maximum concentration of 2 wt %, renders PHBHHx slightly stiffer, but it still retains its ductile nature. As a result, the potential for applications, where flexibility is a necessity, was not compromised. Additionally, it is assumed that important improvements can be further obtained by co-addition of selected plasticizers and talc into PHBHHx, a possibility to achieve a good balance between stiffness and toughness with well-controlled crystallization properties.[40]

CONCLUSIONS

In this study, the performance of ultra-fine talc (median diameter = 1 μm) as a nucleating agent for PHBHHx, as well as the effect of the filler on selected packaging-related properties, was

Table VII. Tensile Properties of PHBHHx/talc Composites

Talc content	Young's modulus (MPa)	Maximum tensile strength (MPa)	Nominal strain at maximum load (%)	Nominal strain at break (%)
0 wt %	804 (±24)	21.5 (±0.4)	6.8 (±0.2)	8.3 (±0.2)
0.5 wt %	838 (±18)	22.0 (±0.2)	6.7 (±0.1)	8.3 (±0.4)
1 wt %	860 (±16)	21.7 (±0.4)	6.4 (±0.1)	8.2 (±0.4)
2 wt %	907 (±20)	21.9 (±0.3)	6.3 (±0.2)	7.9 (±0.2)

comprehensively characterized. A characterization toward a specific application is most often overlooked in studies regarding nucleating agents, but can be of high added value. Ultra-fine talc concentrations of 0.5, 1, and 2 wt % were used.

Via an isothermal and non-isothermal crystallization study, it was proven that ultra-fine talc is an excellent nucleating agent for PHBHHx. Isothermal crystallization half time at 70 °C was reduced by 97%, in comparison to neat PHBHHx by adding 2 wt % ultra-fine talc, which is highly advantageous for the processability of PHBHHx, which is currently one of the main drawbacks of PHBHHx.

Thermal stability was shown to increase slightly, by about 4 °C. Color changes were only minor and a slight increase in opacity from 10.0 to 13.9%, upon addition of 2 wt % ultra-fine talc, was observed. The gas permeability properties (O_2, CO_2, and water vapor), which can be highly important for food packaging applications, of the samples containing 0.5 and 1 wt % of talc were slightly higher than that of neat PHBHHx. The gas permeability upon addition of 2 wt % on the other hand was slightly lower. This unusual trend can be attributed to changes in tortuous path, due to a combinatory effect of smaller spherulites and the presence of impermeable talc particles. It is, however, important to note that all samples were still in the same range of applicability, in terms of food packaging materials.

Overall, it can be concluded that minor concentrations (up to 2 wt %) of ultra-fine talc could be very promising to further enhance the industrial processability of PHBHHx, due to it being a highly efficient nucleating agent. Unlike most nucleating agent studies, specific attention was given to the effect of the nucleating agent on selected end-use properties, related to the application as a packaging material. The PHBHHx matrix was slightly stiffer and causing a minor increase in thermal stability. The addition of highly effective nucleating agents is considered a valuable possibility to improve its processing properties and to expand the applications of this biopolymer, especially if the presence of the particles does not significantly influence any other properties.

It is however important to note that an even more outspoken effect could be achieved by using an ultra-fine talc grade with even smaller particle size, which could render the necessary filler concentration even lower. Also, it can be of high interest to test the applicability of ultra-fine talc as a nucleating agent for other types of polymers. The results presented in this study and literature regarding other polymeric systems lead to believe that ultra-fine talc could be a suitable nucleating agent for a broad array of polymers.

ACKNOWLEDGMENTS

The authors would like to thank J. Put, G. Reggers, and D. Adons for their help with respectively gel permeation chromatography, differential scanning calorimetry, and gas permeability measurements.

REFERENCES

1. Babu, R.; O'Connor, K.; Seeram, R. *Prog. Biomat.* **2013**, *2*, 1.
2. Philip, S.; Keshavarz, T.; Roy, I. *J. Chem. Technol. Biotechnol.* **2007**, *82*, 233.
3. Amass, W.; Amass, A.; Tighe, B. *Polym. Int.* **1998**, *47*, 89.
4. Poirier, Y.; Nawrath, C.; Somerville, C. *Nat. Biotechnol.* **1995**, *13*, 142.
5. Jacquel, N.; Tajima, K.; Nakamura, N.; Miyagawa, T.; Pan, P.; Inoue, Y. *J. Appl. Polym. Sci.* **2009**, *114*, 1287.
6. Liu, W. J.; Yang, H. L.; Wang, Z.; Dong, L. S.; Liu, J. J. *J. Appl. Polym. Sci.* **2002**, *86*, 2145.
7. Qian, J.; Zhu, L.; Zhang, J.; Whitehouse, R. S. *J. Polym. Sci. Part B: Polym. Phys.* **2007**, *45*, 1564.
8. Doi, Y.; Kitamura, S.; Abe, H. *Macromolecules* **1995**, *28*, 4822.
9. Lu, X.; Zhang, J.; Wu, Q.; Chen, G. Q. *FEMS Microbiol. Lett.* **2003**, *221*, 97.
10. Noda, I.; Lindsey, S. B., Caraway, D. In Plastics from Bacteria; Chen, G. G.-Q., Ed.; Springer: Berlin, **2010**; p 237.
11. Zhang, X.; Lin, G.; Abou-Hussein, R.; Hassan, M. K.; Noda, I.; Mark, J. E. *Eur. Polym. J.* **2007**, *43*, 3128.
12. Yu, F.; Pan, P.; Nakamura, N.; Inoue, Y. *Macromol. Mater. Eng.* **2011**, *296*, 103.
13. Leong, Y. W.; Ishak, Z. A. M.; Ariffin, A. *J. Appl. Polym. Sci.* **2004**, *91*, 3327.
14. Mucha, M.; Królikowski, Z. *J. Therm. Anal. Calorim.* **2003**, *74*, 549.
15. Jiang, X. L.; Luo, S. J.; Chen, X. D. *Express Polym. Lett.* **2007**, *1*, 245.
16. Gatta, G. D.; Merlini, M.; Valdrè, G.; Liermann, H. P.; Nénert, G.; Rothkirch, A.; Kahlenberg, V.; Pavese, A. *Phys. Chem. Miner.* **2013**, *40*, 145.
17. Malandrini, H.; Clauss, F.; Partyka, S.; Douillard, J. M. *J. Colloid Interface Sci.* **1997**, *194*, 183.
18. Zazenski, R.; Ashton, W. H.; Briggs, D.; Chudkowski, M.; Kelse, J. W.; Maceachern, L.; McCarthy, E. F.; Nordhauser, M. A.; Roddy, M. T.; Teetsel, N. M.; Wells, A. B.; Gettings, S. D. *Regul. Toxicol. Pharm.* **1995**, *21*, 218.
19. Kai, W.; He, Y.; Inoue, Y. *Polym. Int.* **2005**, *54*, 780.
20. Zhu, C.; Nomura, C. T.; Perrotta, J. A.; Stipanovic, A. J.; Nakas, J. P. *Polym. Test.* **2012**, *31*, 579.
21. Wang, L.; Wang, X.; Zhu, W.; Chen, Z.; Pan, J.; Xu, K. *J. Appl. Polym. Sci.* **2010**, *116*, 1116.
22. Švehlová, V.; Polouček, E. *Angew. Makromol. Chem.* **1994**, *214*, 91.
23. Petchwattana, N.; Covavisaruch, S.; Petthai, S. *Polym. Bull.* **2014**, *71*, 1947.
24. Tábi, T.; Suplicz, A.; Czigány, T.; Kovács, J. *J. Therm. Anal. Calorim.* **2014**, *118*, 1419.
25. DePolo, W. S.; Baird, D. G. *Polym. Compos.* **2009**, *30*, 188.
26. Vandewijngaarden, J.; Wauters, R.; Murariu, M.; Dubois, P.; Carleer, R.; Yperman, J.; D'Haen, J.; Ruttens, B.; Schreurs, S.; Lepot, N.; Peeters, R.; Buntinx, M. *J. Polym. Environ.* **2016**, 1.
27. Zhang, Q.; Liu, Q.; Mark, J. E.; Noda, I. *Appl. Clay Sci.* **2009**, *46*, 51.
28. Zhang, X.; Lin, G.; Abou-Hussein, R.; Allen, W. M.; Noda, I.; Mark, J. E. *J. Macromol. Sci. Part A* **2008**, *45*, 431.

29. Xie, Y.; Kohls, D.; Noda, I.; Schaefer, D. W.; Akpalu, Y. A. *Polymer* **2009**, *50*, 4656.
30. Ding, C.; Cheng, B.; Wu, Q. *J. Therm. Anal. Calorim.* **2011**, *103*, 1001.
31. Bronlund, J. E.; Redding, G. P.; Robertson, T. R. *Packag. Technol. Sci.* **2013**, *27*, 193.
32. Cagnon, T.; Guillaume, C.; Guillard, V.; Gontard, N. *Packag. Technol. Sci.* **2013**, *26*, 137.
33. Kuorwel, K. K.; Cran, M. J.; Sonneveld, K.; Miltz, J.; Bigger, S. W. *Packag. Technol. Sci.* **2013**, *27*, 149.
34. Pan, P.; Shan, G.; Bao, Y.; Weng, Z. *J. Appl. Polym. Sci.* **2013**, *129*, 1374.
35. Pan, P.; Liang, Z.; Nakamura, N.; Miyagawa, T.; Inoue, Y. *Macromol. Biosci.* **2009**, *9*, 5.
36. Vandewijngaarden, J.; Murariu, M.; Dubois, P.; Carleer, R.; Yperman, J.; Adriaensens, P.; Schreurs, S.; Lepot, N.; Peeters, R.; Buntinx, M. *J. Polym. Environ.* **2014**, *22*, 501.
37. Jacquel, N.; Tajima, K.; Nakamura, N.; Kawachi, H.; Pan, P.; Inoue, Y. *J. Appl. Polym. Sci.* **2010**, *115*, 709.
38. Jain, S.; Reddy, M. M.; Mohanty, A. K.; Misra, M.; Ghosh, A. K. *Macromol. Mater. Eng.* **2010**, *295*, 750.
39. Sun, B.; Chuai, C.; Luo, S.; Guo, Y.; Han, C. *J. Polym. Eng.* **2014**, *34*, 379.
40. Shi, X.; Zhang, G.; Phuong, T.; Lazzeri, A. *Molecules* **2015**, *20*, 1579.